Filomat 32:20 (2018), 6937–6951
https://doi.org/10.2298/FIL1820937P

Published by Faculty of Sciences and Mathematics,
University of Niš, Serbia
Available at: http://www.pmf.ni.ac.rs/filomat

Calculation of the Channel Discharge Function for the Generalized Lightning Traveling Current Source Return Stroke Model

Dragan Pavlović[a], Gradimir V. Milovanović[b,c], Jovan Cvetić[a]

[a]*School of Electric Engineering, University of Belgrade, Bulevar Kralja Aleksandra 73*
[b]*Serbian Academy of Sciences and Arts, Kneza Mihaila 35, 11000 Beograd, Serbia*
[c]*University of Niš, Faculty of Sciences and Mathematics, P.O. Box 224, 18000 Niš, Serbia*

Abstract. The generalized lightning traveling current source return stroke model (also called GTCS model) represents generalization of all engineering lightning return stroke models that is generalization of the transmission line (TL models, also called current propagation models) and traveling current source models (TCS models, also known as current generation models). The channel discharge function was introduced and calculated for special cases within the GTCS model. We applied new numerical method for the calculation of the channel discharge function. The proposed method is highly accurate, extremely efficient and relatively simple.

1. Introduction and Preliminaries

The GTCS model has made significant contribution to the study of atmospheric discharge at a time when it was developed [6]. Theoretically, it generalized all TCS models and eliminated many of their shortcomings, such as discontinuity of current and discontinuity of the first derivate of the current at the place of the return stroke current waveform [7]. This model can be observed as an AP model where the charge sections of the corona envelope are discharging one after another when current waveform of the return stroke comes. Each cylindrical section of the corona envelope is a small current source that is activated when the potential of the core is equalized with the potential of the earth after passing return stroke current waveform. According to its concepts, this model is based on TCS models [13], although TL models can be derived from it.

From a mathematical point of view, this article represents a study of the new class of nonlinear Volterra integral equation of the first kind. Problems with these equations are classical problems in numerical analysis and many authors have dealt with them, but only a small number of them succeeded in the process of solving of such an equation with impulse function in the science of lightning [8]. Voltera equations of the

2010 *Mathematics Subject Classification*. Primary 65R20; Secondary 44A10, 44A20, 44A35, 65D30, 78A35
Keywords. channel discharge function, Heidler function, Volterra integral equation, Laplace transform, Meijer G-function, Numerical integration, convolution quadrature method.
Received: 25 November 2018; Accepted: 30 November 2018
Communicated by Miodrag Spalević
The work of the authors was partially supported by the Serbian Ministry of Education, Science and Technological Development, Projects TR-37019 (D. Pavlović and J. Cvetić) and OI-174015 (G.V. Milovanović), as well as by the Serbian Academy of Sciences and Arts (Project Φ-96).
Email addresses: dragan.lab3@etf.bg.ac.rs (Dragan Pavlović), gvm@mi.sanu.ac.rs (Gradimir V. Milovanović), cvetic-j@etf.bg.ac.rs (Jovan Cvetić)

first kind are inherently ill-posed problems, meaning the equation solutions are generally unstable. It means that a small error in the input data can lead to a divergent solution, which significantly complicates the numerical solution of integral equations. Volterra integral equation represents the essence of mathematical models in physics, high voltage engineering, ecology and economy.

The main purpose of this paper is to calculate the channel discharge function $f(t - z/v^*)$ and analyze method, as well as the obtained results. We start with the Volterra integral equation of the first kind

$$i_{\text{cb}}(t) = \int_0^{v^* t} q_0'(z) \frac{\partial}{\partial t} f(t - z/v^*) \, \mathrm{d}z, \tag{1}$$

where $f(t)$ is an unknown function, while the known functions are the channel-base current function i_{cb}, the total line charge density along the channel $q_0'(z)$, the absolute time t, the channel altitude z, the speed of the return stroke v and the reduce return stroke speed v^*.

Using the so-called generalized time u, given by

$$u = t - \frac{z}{v^*}, \quad u \geq 0, \tag{2}$$

we simply write $f(t - z/v^*) = f(u)$. The functions $i_{\text{cb}}(t)$ and $q_0'(z)$ are real physical quantities, and the channel discharge function that we calculate is fictitious physical quantity which are derived from the GTCS model. It presents the sum of all physical processes in the lightning channel during return stroke [5]. We used Heidler function [32] for modeling channel-base current as it is common in the literature. Its shape is given by

$$i_{\text{cb}}(t) = \frac{I_0}{\eta} \cdot \frac{(t/\tau_1)^n}{1 + (t/\tau_1)^n} \mathrm{e}^{-t/\tau_2}. \tag{3}$$

Unknown parameters in Eq. (3) are: I_0 is the maximum value of the current, n is the maximum current steepness, η is a correction factor of the current peak, and τ_1 and τ_2 are time constants determining current rise-time and current decay-time. The values of the parameters in the equation (3) can be obtained from the measurement.

The function in which models charge in lightning channel $q_0'(z)$ was introduced in [5]. Namely, starting from the Heidler function, the basic function for the line charge density was assumed in the form

$$g(z) = \frac{z^m}{\lambda_1^m + z^m} \mathrm{e}^{-z/\lambda_2}, \tag{4}$$

with the parameters given by $m = n$, $\lambda_1 = v^*\tau_1$ and $\lambda_2 = v^*\tau_2$, while the variable z represents the heigh of the channel.

Having known the form of the basis function (4), in general case we can obtain the function of the line charge density as a sum of the basis function and the perturbation of its derivatives,

$$q_0'(z) = Q_0' \left\{ g(z) + \lambda_{d_1} \frac{\mathrm{d}g(z)}{\mathrm{d}z} + \lambda_{d_2} \frac{\mathrm{d}^2 g(z)}{\mathrm{d}z^2} \right\}. \tag{5}$$

The parameters λ_{d_1} and λ_{d_2} can be obtained as $\lambda_{d_1} = v^*\tau_{d_1}$ and $\lambda_{d_2} = (v^*\tau_{d_2})^2$, where τ_{d_1} and τ_{d_2} are time discharge constants for given GTCS model. The parameter Q_0' is the maximum value of the line charge density. The biggest advantage of the function for modeling the charge in the lightning channel (5) in compare to other functions is that it allows to take into account the influence of different charge distribution on physical processes in the lightning channel and on the radiated lightning electromagnetic pulse (LEMP).

The speed of the return stroke v that appeared in the previous expressions is a constant and it is determined based on the optical measurements.

The first step towards precise identification of physical processes in the lightning channel is calculation of the function $f(u)$. According to the physics of electrical discharges, this function must satisfy the following four conditions:

$$f(0) = 0, \tag{6}$$

$$f(u) \geq 0, \quad \text{for } u \geq 0, \tag{7}$$

$$\lim_{u\to\infty} f(u) = 0, \tag{8}$$

$$\frac{\mathrm{d}f(u)}{\mathrm{d}u} \leq 0, \quad \text{for } u \geq u_0, \tag{9}$$

for some $u_0 > 0$.

The second step is connecting the obtained result with the physics of electrical discharges in cylindrical geometry, which will be studied in some other papers.

According to (1), we deal with non-homogeneous Volterra integral equation of the first kind. It can be simplified by introducing the following transformation $f_1(t - z/v^*) = \frac{\partial}{\partial t} f(t - z/v^*)$ in the equation (1), in which (1) becomes

$$i_{\mathrm{cb}}(t) = \int_0^{v^* t} q_0'(z) f_1(t - z/v^*)\,\mathrm{d}z. \tag{10}$$

By a change of variables $z = v^*\tau$, and taking $q_0'(z) = q_0'(v^*\tau) = q(\tau)$ and $i_{\mathrm{cb}}(t)/v^* = i(t)$, the integration in (10) over $[0, v^* t]$ reduces to the interval $(0, t)$, so the equation (10) becomes an equation on convolution type

$$i(t) = \int_0^t q(\tau) f_1(t - \tau)\,\mathrm{d}\tau = \int_0^t q(t - \tau) f_1(\tau)\,\mathrm{d}\tau, \quad t > 0. \tag{11}$$

This type of equations is very sensitive to perturbations in the parameters, which is particularly present herein due to very rapid changes in the functions that appear in this equation. Therefore, its solving is not easy and requires a special treatment. Sometimes, it is necessary to divide the interval into several sub-segments.

2. Methods for Solving Volterra Equation of Convolution Type

In this section we will introduce three methods for solving Volterra's integral equation on convolution type (11):

- Laplace transform method;
- Convolution quadrature method;
- Modified composite trapezoidal formula.

The last of them has recently been considered in [30], including several examples. Therefore, our aim in this section is to present applications of the first two methods and give few typical examples. We consider the method of transformation of Laplace for basic method, which in this case requires the Meier G-functions application.

2.1. Laplace transform method

This is the standard method for finding the solution of the Volterra integral equation of convolution type (11). The Laplace transform of a function $t \mapsto f_1(t)$, defined for all real numbers $t \geq 0$, is the function $F_1(s)$ given by

$$F_1(s) = \mathcal{L}[f_1(t)](s) = \int_0^\infty \mathrm{e}^{-st} f_1(t)\ \mathrm{d}t, \tag{12}$$

and its application to the convolution (11) gives

$$I(s) = Q(s)F_1(s), \tag{13}$$

where $I(s)$ and $Q(s)$ are Laplace transforms of $i(t)$ and $q(t)$.

In order to determine these transforms we need the following integral

$$G_k(\alpha) = \int_0^\infty \mathrm{e}^{-\alpha x} \frac{x^k}{1+x^k}\, \mathrm{d}x \qquad (\operatorname{Re}\alpha > 0,\ k \in \mathbb{N}), \tag{14}$$

which can be expressed in terms of the Meijer G-function, defined by (see [4, p. 207])

$$\begin{aligned} G^{m,n}_{p,q}\left(z \,\middle|\, \begin{matrix} a_1,\dots,a_p \\ b_1,\dots,b_q \end{matrix}\right) &\equiv G^{m,n}_{p,q}\left(z \,\middle|\, \begin{matrix} a_1,\dots,a_n; a_{n+1},\dots,a_p \\ b_1,\dots,b_m; b_{m+1},\dots,b_q \end{matrix}\right) \\ &= \frac{1}{2\pi \mathrm{i}} \int_L \frac{\prod\limits_{\nu=1}^{m} \Gamma(b_\nu - s) \prod\limits_{\nu=1}^{n} \Gamma(1-a_\nu+s)}{\prod\limits_{\nu=m+1}^{q} \Gamma(1-b_\nu+s) \prod\limits_{\nu=n+1}^{p} \Gamma(a_\nu - s)} z^s \,\mathrm{d}s, \end{aligned}$$

where an empty product is interpreted as 1, and parameters a_ν and b_ν are such that no pole of $\Gamma(b_\nu - s)$, $\nu = 1,\dots,m$, coincides with any pole of $\Gamma(1-b_\mu+s)$, $\mu = 1,\dots,n$.

As we can see m and n are such that $1 \le m \le q$ and $1 \le n \le p$. Roughly speaking, the contour L separates the poles of functions $\Gamma(b_1 - s),\dots,\Gamma(b_m - s)$ from the poles of $\Gamma(1-a_1+s),\dots,\Gamma(1-a_n+s)$.

A discussion on three different paths of integration can be found in [4, p. 207]. Notice also that an alternative (equivalent) definition of the Meijer G-function can be done in terms of the inverse Mellin transform (see [31, p. 793]).

Remark 2.1. In the Wolfram Mathematica, the Meijer G-function [34] is implemented as

```
MeijerG[{{a1,...,an},{an1,,...,ap}},{{b1,...,bm},{bm1,...,bq}},z]
```

and it is suitable for both, symbolic and numerical manipulation, and its value can be evaluated with an arbitrary precision. In many special cases, `MeijerG` is automatically converted to other functions.

Lemma 2.2. *Let* $\operatorname{Re}\alpha > 0$ *and* $k \in \mathbb{N}$. *Then*

$$G_k(\alpha) = \int_0^\infty \mathrm{e}^{-\alpha x} \frac{x^k}{1+x^k}\, \mathrm{d}x = \frac{1}{\sqrt{k(2\pi)^{k-1}}} G^{k+1,1}_{1,k+1}\left(\frac{\alpha^k}{k^k} \,\middle|\, \begin{matrix} -\frac{1}{k} \\ -\frac{1}{k}, 0, \frac{1}{k}, \frac{2}{k}, \dots, \frac{k-1}{k} \end{matrix}\right). \tag{15}$$

In fact, this result represents the Laplace transform of the function

$$t \mapsto \psi_k(t) = \begin{cases} 0, & t < 0, \\ \dfrac{t^k}{1+t^k}, & t \ge 0, \end{cases} \tag{16}$$

when $k \in \mathbb{N}$, i.e., $\mathcal{L}[\psi_k(t)](s) = G_k(s)$. According to properties of the Laplace transform, we also have

$$\mathcal{L}\Big[\psi_k(t)\mathrm{e}^{-\gamma t}\Big](s) = G_k(s+\gamma). \tag{17}$$

Now, we are able to find the Laplace transformations for $i(t) = i_{\mathrm{cb}}(t)/v^*$ and $q(t) = q_0'(v * t)$, given by (3) and (5), respectively.

Thus, we have

$$\begin{aligned} I(s)=\mathcal{L}[i(t)](s) &= \frac{I_0}{\eta v^*}\int_0^\infty \mathrm{e}^{-st}\frac{(t/\tau_1)^n}{1+(t/\tau_1)^n}\mathrm{e}^{-t/\tau_2}\,\mathrm{d}t\\ &= \frac{I_0\tau_1}{\eta v^*}\int_0^\infty \mathrm{e}^{-(\tau_1 s+\tau_1/\tau_2)x}\frac{x^n}{1+x^n}\,\mathrm{d}x\\ &= A\tau_1 G_n\Big(\tau_1\big(s+\tau_2^{-1}\big)\Big), \end{aligned} \tag{18}$$

where G_n is given by (15) and the constant A is given by $A=I_0/(\eta v^*)$.

In order to find the Laplace transform of $q(t)$, $Q(s)=\mathcal{L}[q(t)](s)$, we first determine $G(s)=\mathcal{L}[\hat{g}(t)](s)$, where $\hat{g}(t)=g(v^*t)$ and g is defined by (4).

Now we introduce new time constants $\hat{\tau}_1$ and $\hat{\tau}_2$ by

$$\lambda_1=v^*\hat{\tau}_1 \quad\text{and}\quad \lambda_2=v^*\hat{\tau}_2, \tag{19}$$

and by putting $t=\hat{\tau}_1 x$, we have

$$\begin{aligned} G(s) &= \int_0^\infty \mathrm{e}^{-st}\frac{(v^*t)^m}{\lambda_1^m+(v^*t)^m}\mathrm{e}^{-v^*t/\lambda_2}\,\mathrm{d}t\\ &= \int_0^\infty \mathrm{e}^{-st}\frac{(t/\hat{\tau}_1)^m}{1+(t/\hat{\tau}_1)^m}\mathrm{e}^{-t/\hat{\tau}_2}\,\mathrm{d}t\\ &= \hat{\tau}_1\int_0^\infty \mathrm{e}^{-\hat{\tau}_1(s+1/\hat{\tau}_2)x}\frac{x^m}{1+x^m}\,\mathrm{d}x, \end{aligned}$$

i.e.,

$$G(s)=\mathcal{L}[\hat{g}(t)](s)=\hat{\tau}_1 G_m\Big(\hat{\tau}_1\big(s+\hat{\tau}_2^{-1}\big)\Big), \tag{20}$$

where G_m is given by (15).

Now, according to (5), with $g(v^*t)=\hat{g}(t)$, we have

$$q(t)=Q_0'\left\{\hat{g}(t)+\frac{\lambda_{d_1}}{v^*}\,\hat{g}'(t)+\frac{\lambda_{d_2}}{v^{*2}}\,\hat{g}''(t)\right\}.$$

Since $m\ge 1$ and

$$\hat{g}(t)=\frac{(v^*t)^m}{\lambda_1^m+(v^*t)^m}\mathrm{e}^{-v^*t/\lambda_2}=\frac{t^m}{\hat{\tau}_1^m+t^m}\mathrm{e}^{-t/\hat{\tau}_2}\quad\text{and}\quad \hat{g}'(t)=-\frac{1}{\hat{\tau}_2}\,\hat{g}(t)+\frac{m\hat{\tau}_1^m t^{m-1}}{(\hat{\tau}_1^m+t^m)^2}\mathrm{e}^{-t/\hat{\tau}_2}, \tag{21}$$

we conclude that $\hat{g}(0)=0$ and $\hat{g}'(0)=0$ for $m\ge 2$ and $\hat{g}'(0)=1/\hat{\tau}_1$ when $m=1$. Therefore, for the Laplace transform of $q(t)$ we obtain

$$Q(s)=\mathcal{L}[q(t)](s)=Q_0'\left\{G(s)+\frac{\lambda_{d_1}}{v^*}\Big(sG(s)-\hat{g}(0)\Big)+\frac{\lambda_{d_2}}{v^{*2}}\Big(s^2G(s)-s\hat{g}(0)-\hat{g}'(0)\Big)\right\},$$

i.e.,

$$\begin{aligned} Q(s) &= Q_0'\left\{\left(1+\frac{\lambda_{d_1}}{v^*}\,s+\frac{\lambda_{d_2}}{v^{*2}}\,s^2\right)G(s)-\frac{\lambda_{d_2}}{v^{*2}\hat{\tau}_1}\delta_{m,1}\right\}\\ &= Q_0'\left\{\left(1+\frac{\lambda_{d_1}}{v^*}\,s+\frac{\lambda_{d_2}}{v^{*2}}\,s^2\right)\hat{\tau}_1 G_m\Big(\hat{\tau}_1\big(s+\hat{\tau}_2^{-1}\big)\Big)-\frac{\lambda_{d_2}}{v^{*2}\hat{\tau}_1}\delta_{m,1}\right\}, \end{aligned} \tag{22}$$

because of (20). Here, $\delta_{m,1}$ is Kronecker's delta.

Thus, according to (13), (18) and (22), we get the Laplace transform of the solution $t \mapsto f_1(t)$ of the integral equation of convolution type (11) in the form

$$F_1(s) = \mathcal{L}[f_1(t)](s) = \frac{I(s)}{Q(s)} = \frac{A\tau_1 G_n\left(\tau_1\left(s+\tau_2^{-1}\right)\right)}{Q_0'\left\{\left(1+\frac{\lambda_{d_1}}{v^*}\,s+\frac{\lambda_{d_2}}{v^{*2}}\,s^2\right)\hat{\tau}_1 G_m\left(\hat{\tau}_1\left(s+\hat{\tau}_2^{-1}\right)\right)-\frac{\lambda_{d_2}}{v^{*2}\hat{\tau}_1}\delta_{m,1}\right\}}.$$

As before, we can put $\lambda_{d_1} = v^*\tau_{d_1}$ and $\lambda_{d_2} = (v^*\tau_{d_2})^2$, where τ_{d_1} and τ_{d_2} are time discharge constants for given GTCS model. Then, we have

$$F_1(s) = \frac{K\,G_n\left(\tau_1(s+\tau_2^{-1})\right)}{\left(1+\tau_{d_1}s+\tau_{d_2}^2 s^2\right)G_m\left(\hat{\tau}_1(s+\hat{\tau}_2^{-1})\right)-\left(\frac{\tau_{d_2}}{\hat{\tau}_1}\right)^2\delta_{m,1}}, \tag{23}$$

where $K = A(\tau_1/\hat{\tau}_1)/Q_0' = I_0(\tau_1/\hat{\tau}_1)/(\eta v^* Q_0')$.

As we know the Laplace transform $F_1(s)$ is an analytic function in the region $|\arg(s-\sigma)| < \pi - \varphi$, with $\varphi < \pi/2$ and $\sigma \in \mathbb{R}$, and satisfies the condition $|F_1(s)| \le M/|s|^\mu$ for some positive constants M and μ. Then, the inverse transforms of $F_1(s)$ can be done by

$$f_1(t) = \mathcal{L}^{-1}[F_1(s)](t) = \frac{1}{2\pi\mathrm{i}}\int_\Gamma \mathrm{e}^{st}\,F_1(s)\;\mathrm{d}s,$$

where Γ is a curve locates in the analytic region of $F_1(s)$ and can be chosen as running from $\infty\cdot\mathrm{e}^{-\mathrm{i}(\pi-\varphi)}$ to $\infty\cdot\mathrm{e}^{\mathrm{i}(\pi-\varphi)}$ (cf. [17]). In general case, this complex integral cannot be computed in analytic form. In such cases we must use some methods for its approximative computation for a given $t > 0$. Different methods for numerical inversion of the Laplace transform were described in several papers [11], [35], [16], [1], [2], [36], [26], [38], [14], [10], [37], which include Fourier series expansions, Laguerre and Puiseux expansions, a combination of Gaver functionals, different deformations of the Bromwich contour, as well as a method based on Müntz systems (see [24], [25]).

By determining the values $f_1(t_\nu)$ on a particular discrete set $T = \{t_\nu\}_\nu$, we are able to obtain an approximation formula, usually interpolation (cf. [21], [22]), for the inverse transform of $F_1(s)$. Such a solution will be called the "exact" solution of the Volterra integral equation of convolution type (11).

Example 2.3. Now, we consider a typical example of (3), (4), and (5), with the following data:

- $I_0 = 13000\,[\mathrm{A}]$, $\tau_1 = 24\times10^{-8}\,[\mathrm{s}]$, $\tau_2 = 3.4\times10^{-6}\,[\mathrm{s}]$, $\eta = 0.87$, $n = 5$;
- $Q_0' = -1.885\times10^{-4}\,[\mathrm{C/m}]$, $\lambda_1 = 4.5\,[\mathrm{m}]$, $\lambda_2 = 255\,[\mathrm{m}]$, $\lambda_{d_1} = 45\,[\mathrm{m}]$, $\lambda_{d_1} = 0\,[\mathrm{m}]$, $m = 4$,

as well as

$$c = 3\times10^8\,[\mathrm{m/s}],\quad v = \frac{c}{3} = 10^8\,[\mathrm{m/s}],\quad v^* = \frac{v\,c}{v+c} = 7.5\times10^7\,[\mathrm{m/s}].$$

The problem will be considered on the interval $[0, T_{\max}]$, where $T_{\max} = 20\times10^{-6}$ [s].

Thus, in this case, we have

$$i(t) = \frac{I_0}{\eta v^*}\cdot\frac{t^5}{\tau_1^5+t^5}\mathrm{e}^{-t/\tau_2}\quad\text{and}\quad q(t) = \widehat{Q}_0\,\frac{t^3(t^5+a_1t+a_0)}{(t^4+\hat{\tau}_1^4)^2}\mathrm{e}^{-t/\hat{\tau}_2}, \tag{24}$$

where, according to (19), $\hat{\tau}_1 = 6\times10^{-8}$ [s] and $\hat{\tau}_2 = 3.4\times10^{-6}$ [s], as well as

$$\frac{I_0}{\eta v^*} = \frac{13}{65250}\,[\mathrm{C/m}] = 1.992337164750958\times10^{-4}\,[\mathrm{C/m}],\quad \widehat{Q}_0 = -1.552352941176471\times10^{-4}\,[\mathrm{C/m}],$$

$$a_1 = a_1 = 1.296\times10^{-29}\,[\mathrm{s}^4]\quad\text{and}\quad a_0 = 3.776914285714286\times10^{-35}\,[\mathrm{s}^5].$$

Using (23) and Lemma 2.2, we obtain the Laplace transform of $t \mapsto f_1(t)$ in terms of the Mejer function,

$$F_1(s) = \frac{C}{1+\tau_{d_1} s} \cdot \frac{G^{6,1}_{1,6}\left(\frac{\tau_1^5}{3125}(s+\tau_2^{-1})^5 \,\middle|\, \begin{matrix} -\frac{1}{5} \\ -\frac{1}{5}, 0, \frac{1}{5}, \frac{2}{5}, \frac{3}{5}, \frac{4}{5} \end{matrix} \right)}{G^{5,1}_{1,5}\left(\frac{\hat{\tau}_1^4}{256}(s+\hat{\tau}_2^{-1})^4 \,\middle|\, \begin{matrix} -\frac{1}{4} \\ -\frac{1}{4}, 0, \frac{1}{4}, \frac{1}{2}, \frac{3}{4} \end{matrix} \right)}, \tag{25}$$

where

$$C = \frac{K\sqrt{m}}{\sqrt{n(2\pi)^{n-m}}} = \frac{I_0}{\eta v^* Q_0'} \cdot \frac{\tau_1}{\hat{\tau}_1} \sqrt{\frac{m}{n(2\pi)^{n-m}}} = -\frac{6400}{7569}\sqrt{\frac{10}{\pi}} = -1.508573701067213$$

and

$$\tau_{d_1} = 6\times 10^{-7}\,[\mathrm{s}],\ \ \tau_1^5 = 7.962624\times 10^{-34}\,[\mathrm{s}^5],\ \ \hat{\tau}_1^4 = 1.296\times 10^{-29}\,[\mathrm{s}^4],\ \ \tau_2^{-1} = \hat{\tau}_2^{-1} = 294117.6470588235\,[1/\mathrm{s}].$$

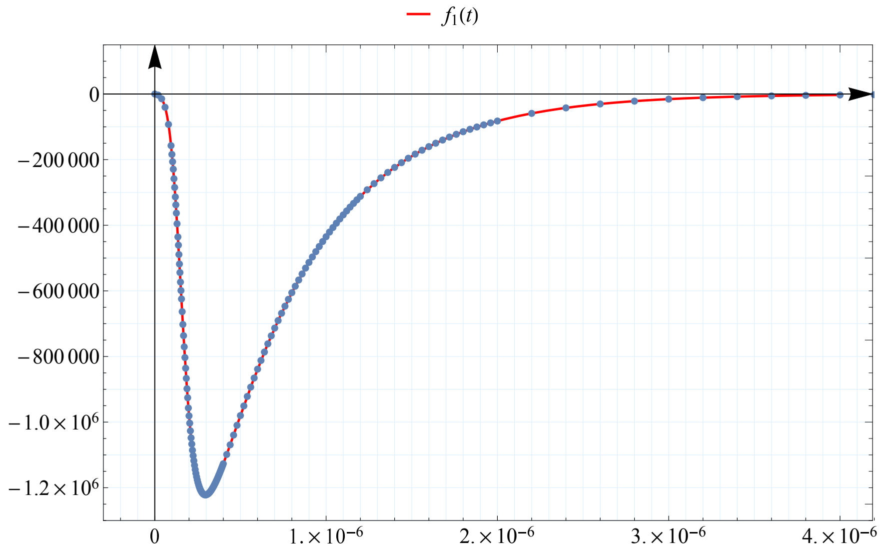

Figure 1: The solution $t \mapsto f_1(t)$ on $[0, T_{\max}/5]$ obtained by numerical inversion of the Laplace transformation using the Gaver method

Applying the Gaver method [11] (see also [36]), we determine the numerical values of $f_1(t)$ for a given $t \in [0, T_{\max}]$. According to the behavior of the function $t \mapsto f_1(t)$, we divide the interval $[0, T_{\max}]$ into six subintervals

$$\left[0, T_{\max}\right] = \left[0, \frac{T_{\max}}{200}\right] \cup \left[\frac{T_{\max}}{200}, \frac{T_{\max}}{50}\right] \cup \left[\frac{T_{\max}}{50}, \frac{3T_{\max}}{50}\right] \cup \left[\frac{3T_{\max}}{50}, \frac{T_{\max}}{10}\right] \cup \left[\frac{T_{\max}}{10}, \frac{T_{\max}}{2}\right] \cup \left[\frac{T_{\max}}{2}, T_{\max}\right],$$

and take in each of these subintervals 6, 75, 40, 20, 40, 25 equidistant points, respectively. The obtained values of the function $f_1(\tau_\nu)$ in these points τ_ν (blue points), as well as the corresponding interpolation function, i.e., the "exact" solution (red line), are presented in Figure 1 on $[0, T_{\max}/5]$.

Finally, we mention that this kind of numerical inversion takes a long time. In our case, it is about one hour and 30 minutes for calculating 206 values in all of 6 subintervals using the Gaver method. Indeed, for calculating one value of $f_1(\tau_\nu)$, the running time is about 26 seconds, so that the total time for all values is about 5356 seconds. The running time is evaluated by the function `Timing` in Mathematica and it includes only CPU time spent in the Mathematica kernel. That kind of work may give different results on different occasions within a session, because of the use of internal system caches. In order to generate worst-case timing results independent of previous computations we used the command `ClearSystemCache[]`. All computations were performed in Mathematica, Ver. 11.12, on MacBook Pro, OS X 10.13.6.

2.2. Convolution quadrature method

Here, we consider a method developed by Lubich [17–19] (see also [33, Chap. 2]). As before, let $F_1(s)$ denote the Laplace transform of $f_1(t)$ in (11), given by (12). In order to describe this convolution quadrature method we note that

$$q(t-\tau) = \mathcal{L}^{-1}\left[\mathrm{e}^{-s\tau}Q(s)\right] = \frac{1}{2\pi\mathrm{i}}\int_\Gamma \mathrm{e}^{s(t-\tau)}Q(s)\,\mathrm{d}s,$$

where $Q(s) = \mathcal{L}[q(t)](s)$. Substituting it into (11) we can get

$$\begin{aligned} i(t) &= \int_0^t \left(\frac{1}{2\pi\mathrm{i}}\int_\Gamma \mathrm{e}^{s(t-\tau)}Q(s)\,\mathrm{d}s\right) f_1(\tau)\,\mathrm{d}\tau \\ &= \frac{1}{2\pi\mathrm{i}}\int_\Gamma Q(s)\left(\int_0^t \mathrm{e}^{s(t-\tau)}f_1(\tau)\,\mathrm{d}\tau\right)\mathrm{d}s \\ &= \frac{1}{2\pi\mathrm{i}}\int_\Gamma Q(s)\varphi(t,s)\,\mathrm{d}s, \end{aligned} \tag{26}$$

where

$$\varphi(t,s) = \int_0^t \mathrm{e}^{s(t-\tau)}f_1(\tau)\,\mathrm{d}\tau.$$

It is easy to see that this function $t \mapsto \varphi(t,s)$ (in the first variable) satisfies the following initial (Cauchy) value problem

$$\varphi'(t,s) = s\,\varphi(t,s) + f_1(t), \quad \varphi(0,s) = 0. \tag{27}$$

After discretizing the time with equal steps $\Delta t = h$, i.e., $t_n = nh$, $n = 0, 1, \ldots$, the solution of (27) at these points $\varphi(nh,s)$ can be approximated by the discrete values y_n obtained by some multistep method

$$\sum_{\nu=0}^{k}\alpha_\nu y_{n+\nu} = h\sum_{\nu=0}^{k}\beta_\nu[sy_{n+\nu} + f_1((n+\nu)h)], \quad n \geq -k, \tag{28}$$

where $y_{-k} = \cdots = y_{-1} = 0$ and $f_1(t) = 0$ for $t < 0$. Details on multistep methods can be found in [23, Ch. 8.2].

Multiplying (28) by ζ^{n+k} and summing over $n \in \mathbb{N}_0$, we get

$$(\alpha_0\zeta^k + \alpha_1\zeta^{k-1} + \cdots + \alpha_k)\mathbf{y}(\zeta) = h(\beta_0\zeta^k + \beta_1\zeta^{k-1} + \cdots + \beta_k)[s\mathbf{y}(\zeta) + \mathbf{f}_1(\zeta)],$$

where $\mathbf{y}(\zeta) = \sum_{n=0}^{\infty} y_n\zeta^n$ and $\mathbf{f}_1(\zeta) = \sum_{n=0}^{\infty} f_1(nh)\zeta^n$. Introducing $\delta(\zeta)$ as

$$\delta(\zeta) = \frac{\alpha_0\zeta^k + \alpha_1\zeta^{k-1} + \cdots + \alpha_k}{\beta_0\zeta^k + \beta_1\zeta^{k-1} + \cdots + \beta_k},$$

we get $\mathbf{y}(\zeta) = [\delta(\zeta)/h - s]^{-1}\mathbf{f}_1(\zeta)$. Thus, in this way, an approximation of $\varphi(t,s)$ at $t = nh$, denoted by y_n, can be obtained as the n-th coefficient of the power series $[\delta(\zeta)/h - s]^{-1}\mathbf{f}_1(\zeta) = \sum_{n=0}^{\infty} y_n\zeta^n$. Furthermore, according to (26) and using Cauchy's integral formula, we can get the corresponding approximation of $i(t)$ at $t = nh$.

Since $Q(s)$ is analytic in the inside region of the curve Γ, we have

$$\frac{1}{2\pi\mathrm{i}}\int_\Gamma Q(s)\left(\frac{\delta(\zeta)}{h} - s\right)^{-1}\mathbf{f}_1(\zeta)\,\mathrm{d}s = Q\left(\frac{\delta(\zeta)}{h}\right)\mathbf{f}_1(\zeta).$$

Assuming the power Taylor expansion

$$Q\left(\frac{\delta(\zeta)}{h}\right) = \sum_{j=0}^{\infty} \omega_j(h)\zeta^j,$$

the right hand side in the previous formula becomes

$$Q\left(\frac{\delta(\zeta)}{h}\right)\mathbf{f}_1(\zeta) = \left(\sum_{j=0}^{\infty} \omega_j(h)\zeta^j\right)\left(\sum_{n=0}^{\infty} f_1(nh)\zeta^n\right) = \sum_{n=0}^{\infty}\left(\sum_{j=0}^{n} \omega_j(h) f_1(nh-jh)\right).$$

The coefficients $\omega_j(h)$ can be expressed as

$$\omega_j(h) = \frac{1}{2\pi \mathrm{i}} \int_{|z|=\rho} Q\left(\frac{\delta(z)}{h}\right) z^{-j-1}\,\mathrm{d}z, \tag{29}$$

where ρ is sufficiently small radius such that the disk $|z| \le \rho$ belongs to the analytic region of the function $z \mapsto Q(\delta(z)/h)$.

Thus, Lubich's convolution quadrature method can be expressed in the form

$$\int_0^t q(\tau) f_1(t-\tau)\,\mathrm{d}\tau = \sum_{0\le jh\le t} \omega_j(h) f_1(t-jh) + R(t; f_1), \quad t \ge 0, \tag{30}$$

where $R(t; f_1)$ is the corresponding remainder term.

The coefficients $\omega_j(h)$ can be calculated numerically, taking $z = \rho \mathrm{e}^{\mathrm{i}\theta}$ in (29) and applying the composite trapezoidal rule to 2π-periodic function $\theta \mapsto Q\left(h^{-1}\delta(\rho\mathrm{e}^{\mathrm{i}\theta})\right)\mathrm{e}^{-\mathrm{i}j\theta}$ in M points,

$$\omega_j(h) = \frac{\rho^{-j}}{2\pi} \int_0^{2\pi} Q\left(h^{-1}\delta(\rho\mathrm{e}^{\mathrm{i}\theta})\right)\mathrm{e}^{-\mathrm{i}j\theta}\,\mathrm{d}\theta \approx \frac{\rho^{-j}}{M} \sum_{\nu=0}^{M-1} Q\left(h^{-1}\delta(\rho\mathrm{e}^{\mathrm{i}2\pi\nu/M})\right)\mathrm{e}^{-\mathrm{i}2\pi\nu j/M}, \quad j = 0, 1, \ldots, n.$$

Remark 2.4. In the recent paper, Ma and Liu [20] have used $M = 10n$, $\rho^n = \sqrt{\varepsilon}$, and $\varepsilon = 10^{-16}$, in order to obtain a precision of order $O(\sqrt{\varepsilon})$. The computation complexity by FFT has been $O(n \log n)$.

An alternative method for calculating quadrature weights $\omega_j(h)$ can be done in the following form (cf. [3], [9], [20])

$$\omega_j(h) = \int_0^{\infty} q(t)\phi_j(t/h)\,\mathrm{d}t, \tag{31}$$

using basis functions $\phi_j(t)$, $j = 0, 1, 2, \ldots$, given by the generating function (see [3, Eq. (3.1)])

$$\mathrm{e}^{-\delta(\zeta)t} = \sum_{j=0}^{\infty} \phi_j(t)\zeta^j.$$

Explicit formulas for $\omega_j(h)$ based on the backward difference formulas of the first and second order (BDF1 and BDF2) were used in [28] and [12].

Since $\delta(\zeta) = \sum_{j=1}^{k} \frac{1}{j}(1-\zeta)^j$, $k = 1, \ldots, 6$, for BDF1 ($k = 1$) we have

$$\mathrm{e}^{-(1-\zeta)t} = \mathrm{e}^{-t} \sum_{j=0}^{\infty} \frac{t^j \zeta^j}{j!},$$

i.e., $\phi_j(t) = \mathrm{e}^{-t} t^j / j!$, $j = 0, 1, 2, \ldots$ (known as Erlang functions in statistics). For BDF2 ($k = 2$), we have

$$\mathrm{e}^{-\frac{1}{2}(3-4\zeta+\zeta^2)t} = \mathrm{e}^{-3t/2} \sum_{j=0}^{\infty} \frac{H_j(\sqrt{2t})}{j!} \left(\frac{t}{2}\right)^{j/2} \zeta^j,$$

where H_j is the Hermite polynomial of degree j, so that the basis functions are

$$\phi_0(t) = \mathrm{e}^{-3t/2}, \quad \phi_1(t) = 2\mathrm{e}^{-3t/2} t, \quad \phi_2(t) = \frac{1}{2}\mathrm{e}^{-3t/2} t(4t-1), \quad \phi_3(t) = \frac{1}{3}\mathrm{e}^{-3t/2} t^2(4t-3),$$

$$\phi_4(t) = \frac{1}{24}\mathrm{e}^{-3t/2} t^2 \left(16t^2 - 24t + 3\right), \quad \phi_5(t) = \frac{1}{60}\mathrm{e}^{-3t/2} t^3 \left(16t^2 - 40t + 15\right),$$

$$\phi_6(t) = \frac{1}{720}\mathrm{e}^{-3t/2} t^3 \left(64t^3 - 240t^2 + 180t - 15\right), \quad \phi_7(t) = \frac{1}{2520}\mathrm{e}^{-3t/2} t^4 \left(64t^3 - 336t^2 + 420t - 105\right),$$

$$\phi_8(t) = \frac{1}{40320}\mathrm{e}^{-3t/2} t^4 \left(256t^4 - 1792t^3 + 3360t^2 - 1680t + 105\right),$$

$$\phi_9(t) = \frac{1}{181440}\mathrm{e}^{-3t/2} t^5 \left(256t^4 - 2304t^3 + 6048t^2 - 5040t + 945\right),$$

$$\phi_{10}(t) = \frac{1}{3628800}\mathrm{e}^{-3t/2} t^5 \left(1024t^5 - 11520t^4 + 40320t^3 - 50400t^2 + 18900t - 945\right), \quad \text{etc.}$$

These basis functions $\phi_j(t)$, $j = 0, 1, \ldots, 8$, for $k = 1$ and $k = 2$, are presented in Figure 2. In a similar way, we can get the basis functions for $k \geq 3$.

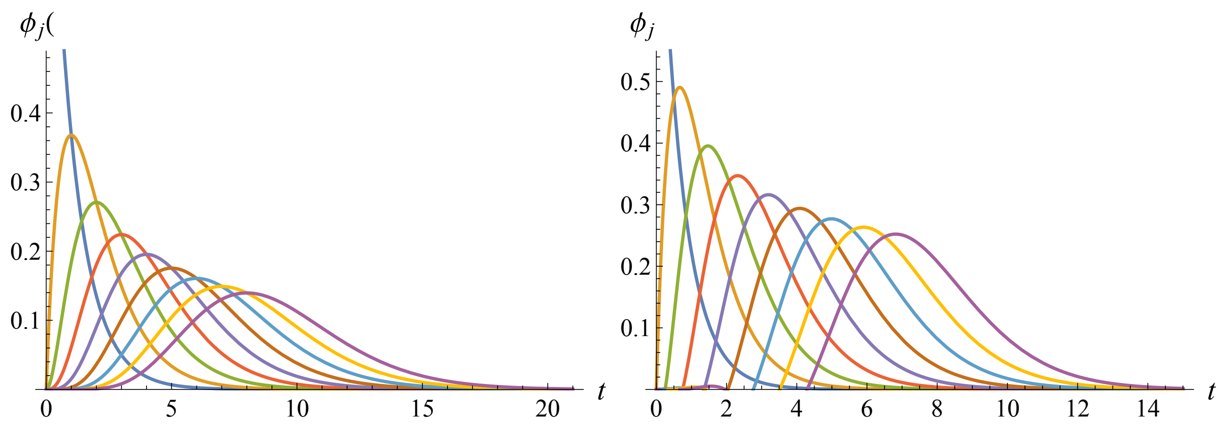

Figure 2: Basis functions $\phi_j(t)$, $j = 0, 1, \ldots, 8$, for BDF1 (left) and BDF2 (right)

The main problem in numerical computation of the quadrature weights $\omega_j(h)$ given by (31) can be slow convergence of the corresponding quadrature rule, due to the proximity of the singularities of the function $t \mapsto q(t)$ around the origin $t = 0$. According to (21), with (19), we can see that the extension of the function $t \mapsto \hat{g}(t)$ to the complex plane $\mathbb{C}$ has some singularities at the points $\hat{\tau}_1 \exp\left(\mathrm{i}\frac{(2k+1)\pi}{m}\right)$, $k = 0, 1, \ldots, m-1$. These singularities are also present in the function $t \mapsto q(t)$ (extended to $\mathbb{C}$), only with a higher order. As a suitable transformation for the elimination of singularities in the integration process can be taken

$$t = \hat{\tau}_1 \sinh^{2/m} \xi \qquad \left(\mathrm{d}t = \frac{2\hat{\tau}_1}{m} \sinh^{2/m-1} \xi \cosh \xi \, \mathrm{d}\xi\right). \tag{32}$$

Example 2.5. We consider again the same problem as in Example 2.3, but to solve it we use the convolution quadrature method. Taking the simplest basis functions (BDF1) $\phi_j(t) = \mathrm{e}^{-t}t^j/j!$, $j = 0, 1, 2, \ldots$, we can calculate the quadrature weights $\omega_j(h)$ using (31) and (24),

$$\omega_j(h) = \int_0^\infty \widehat{Q}_0 \frac{t^3(t^5 + a_1 t + a_0)}{(t^4 + \hat{\tau}_1^4)^2} \mathrm{e}^{-t/\hat{\tau}_2} \left(\frac{t}{h}\right)^j \frac{\mathrm{e}^{-t/h}}{j!}\,\mathrm{d}t, \quad j = 0, 1, \ldots ,$$

i.e.,

$$\omega_j(h) = \frac{\widehat{Q}_0}{j!h^j} \int_0^\infty \frac{t^{j+3}(t^5 + a_1 t + a_0)}{(t^4 + \hat{\tau}_1^4)^2} \mathrm{e}^{-(h^{-1}+\hat{\tau}_2^{-1})t}\,\mathrm{d}t, \quad j = 0, 1, \ldots .$$

Four singularities near origin, $6 \times 10^{-8} \exp\left(\mathrm{i}\frac{(2k+1)\pi}{4}\right)$, $k = 0, 1, 2, 3$, can be eliminated by using (32), so that the last integrals become

$$\omega_j(h) = \frac{\widehat{Q}_0 \hat{\tau}_1^{j+1}}{2j!h^j} \int_0^\infty \frac{\Psi_j\left(\sqrt{\sinh \xi}\right)}{\cosh^3 \xi} \mathrm{e}^{-(h^{-1}+\hat{\tau}_2^{-1})\hat{\tau}_1\sqrt{\sinh \xi}}\,\mathrm{d}\xi = -\int_0^\infty \Phi_j(\xi; h)\,\mathrm{d}\xi, \quad j = 0, 1, \ldots , \tag{33}$$

where

$$\Psi_j(z) = z^{j+2}(z^5 + b_1 z + b_0), \quad b_1 = \frac{a_1}{\hat{\tau}_1^4} = 1, \quad b_0 = \frac{a_0}{\hat{\tau}_1^5} = \frac{340}{7} = 48.57142857142857.$$

The functions $\xi \mapsto \Phi_j(\xi; h)$ for different order j and a fixed h ($= 1.5625 \times 10^{-8}$ [s]) are positive and presented in Fig. 3. (We note that $\omega_j(h) < 0$, because of $\widehat{Q}_0 < 0$.)

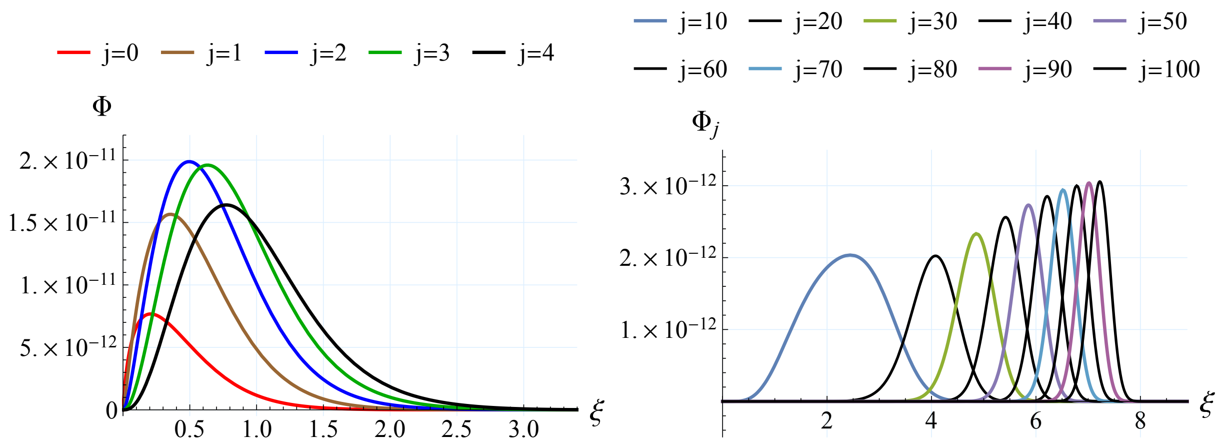

Figure 3: The functions $\xi \mapsto \Phi_j(\xi; h)$ for $j = 0(1)4$ (left) and $j = 10(10)100$ (right) and $h = 1.5625 \times 10^{-8}$ [s]

For calculating these integrals we can use the exponential transformation $\xi = \exp\left(\frac{\pi}{2}\sinh x\right)$ to transform them to integrals over $(-\infty, \infty)$ and then, it is enough to apply the composite trapezoidal rule on a finite interval (cf. [29], [27]). In our case, for calculating the integrals $\omega_j(h)$ in (33) we used the command `NIntegrate` in Mathematica, with the options `Method->"DoubleExponential"` and `WorkingPrecision -> WP`, where `WP` is a given working precision. The method is much faster than the Laplace transform method and it does not use special functions like the Meijer G-function. For example, for calculating one of integrals in (33). for $j = 100$ and $h = 10^{-10}$, the running time is 11 ms (20 ms) if `WP=20` (`WP=50`).

For a given $h > 0$ we can compute the convolution weights $\omega_j(h)$, $j = 0, 1, \ldots, n$, and then we approximate the convolution integral in (11) at the points $t = t_k = kh$, $k = 0, 1, \ldots, n$, by the convolution quadrature (30).

Thus,

$$i_k = i(t_k) = \sum_{j=0}^{k} \omega_j(h) f_1(t_{k-j}) + R(t_k; f_1), \quad k = 0, 1, \dots, n.$$

Omiting $R(t_k; f_1)$ and putting $f_1(kh) \equiv \bar{f}_k$, $k = 0, 1, \dots, n$, we obtain the following triangular system of linear equations,

$$\begin{aligned} i_0 &= \omega_0(h)\bar{f}_0, \\ i_1 &= \omega_0(h)\bar{f}_1 + \omega_1(h)\bar{f}_0, \\ i_2 &= \omega_0(h)\bar{f}_2 + \omega_1(h)\bar{f}_1 + \omega_2(h)\bar{f}_0, \\ &\vdots \\ i_n &= \omega_0(h)\bar{f}_n + \omega_1(h)\bar{f}_{n-1} + \cdots + \omega_n(h)\bar{f}_0. \end{aligned} \tag{34}$$

In our case, taking $h = 1.5 \times 10^{-8}$ [s] and the equidistant points $t_k = kh$, $k = 0, 1, \dots$, on $[0, T_{\max}/8] = [0, 2.4 \times 10^{-6}]$, we can get an approximate solution of $t \mapsto f_1(t)$. Namely, by solving (33) we obtain approximate values $\bar{f}_k, k = 0, 1, \dots, n$, of $f_1(t)$ at the points $t = t_k = kh, k = 0, 1, \dots, n$. Its interpolation function is displayed in Fig. 4, together with the "exact" function obtained by the inverse Laplace transformation. Based on these graphics, we can notice that the corresponding curves differ in their initial parts when t is small (before its minimum).

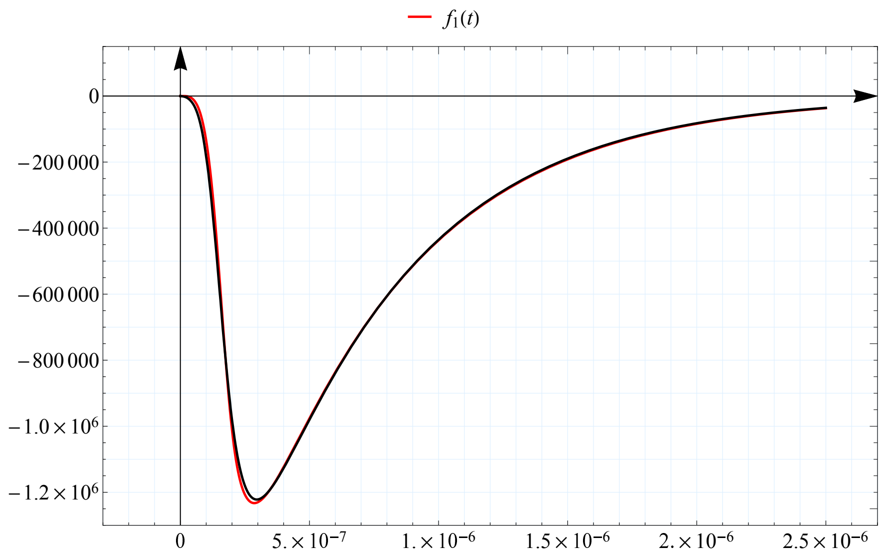

Figure 4: Approximate solution of $f_1(t)$ obtained by the convolution quadrature method for $h = 1.5 \times 10^{-8}$ [s] (red line) and "exact" solution (black line) on $[0, T_{\max}/8]$

The corresponding absolute errors for three different values of h (15, 3, and 1 [ns]) are given in Fig. 5 (left). As we can see an satisfactory result (e.g. when the maximal absolute error is less than 6000 [1/s]) is obtained for $h = 10^{-9}$ [s] (green line).

A better approximation can be obtained by using the basis functions of higher order in (31). For example, if we apply the second order basis functions (BDF2), $\phi_j(t) = \frac{1}{j!} e^{-3t/2} H_j(\sqrt{2t}) \left(\frac{t}{2}\right)^{j/2}$, $j \geq 0$, the absolute error in the corresponding approximation of $f_1(t)$ on $[0, T_{\max}/100] = [0, 2 \times 10^{-7}]$ for two different values of h is presented in Fig. 5 (right). We see that the maximal absolute error is about 4000 [1/s] (blue line) when $h = 2 \times 10^{-9}$ [s].

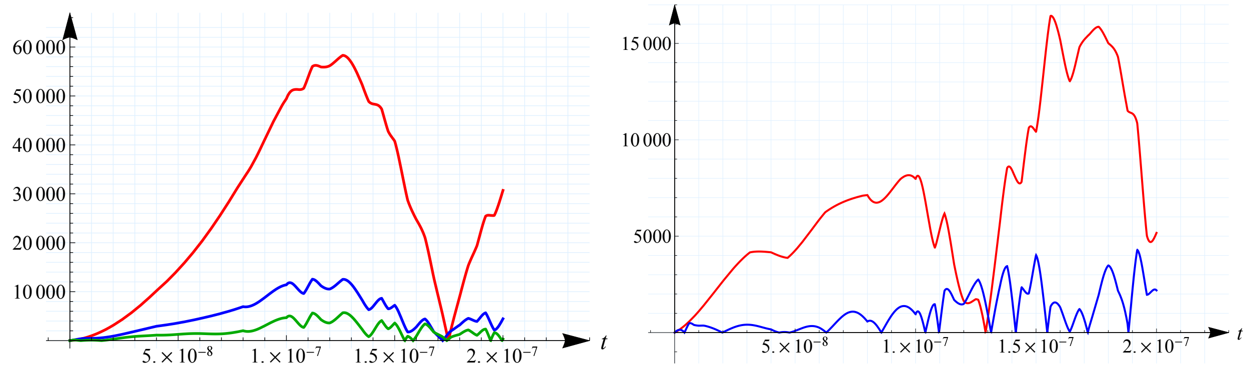

Figure 5: Absolute error in the approximate solution of $t \mapsto f_1(t)$ for BDF1 with $h = 1.5 \times 10^{-8}$ [s] (red line), $h = 3 \times 10^{-9}$ [s] (blue line) and $h = 10^{-9}$ [s] (green line) (left) and for BDF2 with $h = 1.5 \times 10^{-8}$ [s] (red line) and $h = 2 \times 10^{-9}$ [s] (blue line) (right)

Now, we consider this problem on the interval $[0, 3 \times 10^{-7}]$, where the deviations are greatest. With $t \mapsto \bar{f}_h(t)$ we denote the solution (interpolation function) obtained by the convolution quadrature formula (30) based on BDF1 with a step h, and the corresponding convolution integral denote by $i_h(t)$, i.e.,

$$i_h(t) = \int_0^t q(t)\bar{f}_h(t-\tau)\,\mathrm{d}\tau,$$

for whose calculation we can again apply the convolution quadrature method, but with a sufficiently small step h (e.g., $h = 5 \times 10^{-10}$ [s]).

The function $t \mapsto i_h(t)$ for three different values of h ($h_1 = 1.5 \times 10^{-8}$ [s], $h_2 = 3 \times 10^{-9}$ [s] and $h_3 = 10^{-9}$ [s]), as well as $t \mapsto i(t)$ (black line), are presented in Fig. 6 (left). We can see that the graphics of $i_h(t)$ for $h = h_2$ and $h = h_3$ are almost the same as one of $i(t)$. The corresponding residual function $R_h(t) = i_h(t) - i(t)$, i.e., the difference between the approximation $i_h(t)$ and the given function $i(t)$, is displayed in Figure 6 (right) for the same three values of h.

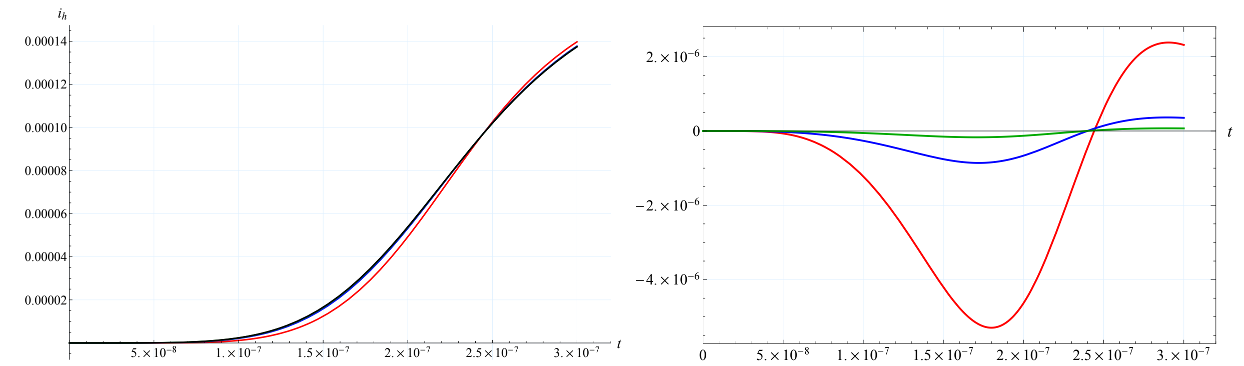

Figure 6: Graphics of the functions $t \mapsto i_h(t)$ for three different values of h (1.5×10^{-8} [s] (red line), 3×10^{-9} [s] (blue line) and 10^{-9} [s] (green line)) and $t \mapsto i(t)$ (black line) (left) and the corresponding residual functions $t \mapsto R_h(t)$ (right)

Finally, the channel discharge function $t \mapsto f(t)$ can be obtained from $f_1(t)$ as

$$f(t) = 1 + \int_0^t f_1(\tau)\,\mathrm{d}\tau.$$

Its graphics is presented in Figure 7.

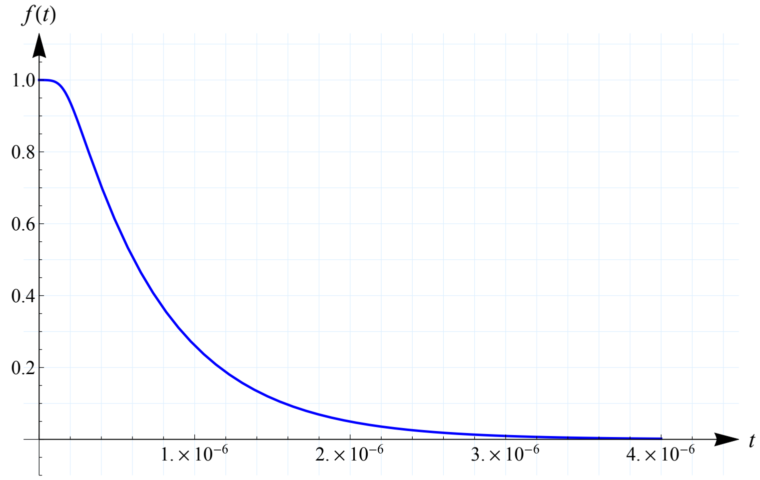

Figure 7: Graphics of the channel discharge function $t \mapsto f(t)$

3. Conclusion

In this paper we proposed and analyzed a precise, efficient and relatively simple method for solving an integral equation of the form (1). Compared to the standard Laplace transformation method, the convolution quadrature method based on the BDF-functions and the calculation of the quadrature weights by (31), including the transformation (32) for eliminating singularities, has several advantages. As we mentioned, the method is much faster than the Laplace transform method and it does not use special functions like the Meijer G-function.

Calculating the channel discharge function opens the way to many calculations in the physics of electrical discharges and power engineering.

References

[1] J. Abate, P.P. Valkó, Multi-precision Laplace transform inversion, Int. J. Numer. Meth. Eng. **60** (2004), 979–993.
[2] J. Abate, W. Whitt, A unified framework for numerically inverting Laplace transforms, INFORMS J. Comput. **18** (2006), no. 4, 408–421.
[3] L. Banjai, Multistep and multistage convolution quadrature for the wave equation: algorithms and experiments, SIAM J. Sci. Comput. **32**, no. 5 (2010), 2964–2994.
[4] H. Bateman, A. Erdélyi, Higher Transcendental Functions, Vol. I, Krieger, New York, 1981.
[5] J.M. Cvetic, Model povratnog udara atmosferskog pražnjenja sa specificiranom strujom u tački udara i raspodelom naelektrisanja duž kanala, doktorska disertacija, Elektrotehnički fakultet Univerziteta u Beogradu, Srbija, 1996.
[6] J.M. Cvetic, B.V. Stanic, An improved return stroke model with specified channel-base current and charge distribution along lightning channel, in: International Conference on Electromagnetics in Advanced Application (ICEAA), Torino, Italy, 1995.
[7] J.M. Cvetic, B.V. Stanic, LEMP calculation usingan improved return stroke model. in: Proc. 12th Int. Symp. on Electromagnetic Compatibility, Zürich, 1997, pp. 77–82.
[8] J.M. Cvetic, B.V. Stanic, F. Heidler, Behavior of the rise and fall characteristics of the channel discharge function for the GTCS return stroke model, in: 15th International Zurich Symposium and Technical Exhibition on EMC, Zürich, 2003, pp. 557–560.
[9] P.J. Davies, D.B. Duncan, Convolution spline approximations for time domain boundary integral equations, J. Integral Equ. Appl. **26** (2014), 369–412.
[10] B. Dingfelder, J.A.C. Weideman, An improved Talbot method for numerical Laplace transform inversion, Numer. Algorithms **68** (2015), 167–183.
[11] D.P. Gaver, Jr., Observing stochastic processes and approximate transform inversion, Oper. Res. **14** (1966), 444–459.
[12] W. Hackbusch, W. Kress, S.A. Sauter, Sparse convolution quadrature for time domain boundary integral formulations of the wave equation, IMA J. Numer. Anal. **29** (2009), 158–179.
[13] F. Heidler, TCS model for LEMP calculation, in: 6th Symposium on EMC, Zürich, 1985, pp. 175–162.
[14] K.L. Kuhlman, Review of inverse Laplace transform algorithms for Laplace-space numerical approaches, Numer. Algorithms **63** (2013), 339–355.
[15] P.K. Kythe, P. Puri, Computational Methods for Linear Integral Equations, Boston, USA, Birkhäuser, 2002.

[16] J. Lyness, G. Giunta, A modification of the Weeks method for numerical inversion of the Laplace transform, Math. Comput. **47**(175) (1986), 313–322.
[17] C. Lubich, Convolution quadrature and discretized operational calculus. I, Numer. Math. **52** (1988), 129–145.
[18] C. Lubich, Convolution quadrature and discretized operational calculus. II, Numer. Math. **52** (1988), 413–425.
[19] C. Lubich, convolution quadrature revisited, BIT Numer. Math. **44** (2004), 503–514.
[20] J. Ma, H. Liu, On the convolution quadrature rule for integral transforms with oscillatory Bessel kernels, Symmetry **10**, no. 7: 239 (2018), 15 pp.
[21] G. Mastroianni, G.V. Milovanović, Interpolation Processes: Basic Theory and Applications, Springer, Berlin – Heidelberg, 2008.
[22] G.V. Milovanović, Numerička analiza II, Naučna knjiga, Beograd, 1991.
[23] G.V. Milovanović, Numerička analiza III, Naučna knjiga, Beograd, 1991.
[24] G. V. Milovanović, Müntz orthogonal polynomials and their numerical evaluation, In: Applications and Computation of Orthogonal Polynomials (W. Gautschi, G.H. Golub, and G. Opfer, eds.), pp. 179–194, ISNM, Vol. 131, Birkhäuser, Basel, 1999.
[25] G.V. Milovanović, A.S. Cvetković, Gaussian type quadrature rules for Müntz systems, SIAM J. Sci. Comput. **27** (2005), 893–913.
[26] G.V. Milovanović, A.S. Cvetković, Numerical inversion of the Laplace transform, Facta Univ. Ser. Elec. Energ. **18** (2005), 515–530.
[27] G. Monegato, L. Scuderi, Quadrature rules for unbounded intervals and their application to integral equations, In: Approximation and Computation: In Honor of Gradimir V. Milovanović (W. Gautschi, G. Mastroianni, Th.M. Rassias, eds.), Springer Optimization and its Applications, Vol. 42, Springer, New York, 2011, pp. 185–208.
[28] G. Monegato, L. Scuderi, M.P. Stanic, Lubich convolution quadratures and their application to problems described by space-time BIEs, Numer. Algorithms **56** (2011), 405–436.
[29] M. Mori, Quadrature formulas obtained by variable transformation and DE-rule, J. Comput. Appl. Math. **12&13** (1985), 119–130.
[30] D. Pavlović, G. Milovanović, J. Cvetić, N. Mijajlović, M. Ignjatović, Numerical solution of Volterra integral equation of first kind for GTCS Return Stroke Model, In: Proceedings of Papers, 61$^{\text{st}}$ Conference ETRAN (Kladovo, June 5–8, 2017), pp. AP1.3.1–5, ETRAN Society, Belgrade, Academic Mind, Belgrade 2017 (Serbian).
[31] P. Prudnikov, O.I. Marichev, Yu.A. Brychkov, Integrals and Series, Vol. 3: More Special Functions, Gordon and Breach, Newark, NJ, 1990.
[32] V.A. Rakov, M.A. Uman, Lightning: Physics and Effects, Cambridge University Press, 2003.
[33] M. Schanz, Wave Propagation in Viscoelastic and Poroelastic Continua: A Boundary Element Approach, Springer-Verlag, Berlin – Heidelberg – New York, 2001.
[34] The Wolfram Functions Site, 2008. [Online] Available: http:/functions.wolfram.com.
[35] A. Talbot, The accurate numerical inversion of Laplace transforms, IMA J. Appl. Math. **23** (1979), 97–120.
[36] P. P. Valkó, J. Abate, Comparison of sequence accelerators for the Gaver method of numerical Laplace transform inversion, Comput. Math. Appl. **48** (2004), 629–636.
[37] T. Wang, Y. Gu, Z. Zhang, An algorithm for the inversion of Laplace transforms using Puiseux expansions, Numer. Algorithms **78** (2018), 107–132.
[38] J.A.C. Weideman, L.N. Trefethen, Parabolic and hyperbolic contours for computing the Bromwich integral, Math. Comput. **76** (2007), 1341–1356.